Hydrogen Bonding and Distance Studies of Amino Acids and Peptides Using Solid State 2D $^{1}H-^{13}C$ Heteronuclear Correlation Spectra

Zhengtian Gu,[†] Cynthia F. Ridenour,[‡] Charles E. Bronnimann,[‡] Takashi Iwashita,[†,§] and Ann McDermott*[,†]

Contribution from the Department of Chemistry, Columbia University, New York, New York 10027, and Otsuka Electronics, Inc., 2555 Midpoint Drive, Fort Collins, Colorado 80525

Received June 28, 1995[⊗]

Abstract: Solid state $^{13}C-^{1}H$ 2D HETeronuclear CORrelation spectra (Caravatti, P.; Bodenhausen, G.; Ernst, R. R. *Chem. Phys. Lett.* **1982**, *89*, 363−367. Roberts, J. E.; Vega, S.; Griffin, R. G. *J. Am. Chem. Soc.* **1984**, *106*, 2506−2512) are reported for many amino acids and peptides with ^{13}C isotopic composition at natural abundance. These HETCOR spectra often have multiple proton cross peaks for each carbon, and these cross peaks can be extremely helpful for assigning the spectrum. Apart from peaks due to groups that have a lot of motion, the peak volumes correlate with C−H distance and can be used to estimate distances with standard derivation of 0.2 Å; the longest distances for which cross peaks are visible is 3 Å. The HECTOR pulse sequence also appears to be very useful for studying hydrogen bonding interactions, since the distances for most of C−O···H−X hydrogen bond pairs are within the range that is observable by HETCOR.

Introduction

Solid state nuclear magnetic resonance (SSNMR) spectroscopy has been extensively used to investigate biological systems, with most studies focusing on the well-resolved ^{13}C, ^{15}N, or ^{31}P spectra.[1−4] The resolution of proton SSNMR spectra is poor due to very strong dipole−dipole coupling between protons which results in extremely broad lines. On the other hand, the information available from proton NMR could be very useful for studying ionizable groups involved in hydrogen bonding or proton transfer reactions. Several methods have been developed to increase the resolution and decrease the line width of proton spectra. Among those are the combined rotation and multiple pulse spectroscopy (CRAMPS)[5−7] and magnetic dilution of proton by deuteration.[8,9] However, the resolution is never sufficient for site specific assignments of proteins.

A useful approach is to try to correlate the partially narrowed proton resonance to the nearby heteronuclei. Two general types of 2D heteronuclear SSNMR experiments involving protons have been proposed. The first type includes methods for correlating dipolar couplings and chemical shifts[10] which can give very accurate bond distances. The second type includes heteronuclear correlation methods (HETCOR),[11−13] which correlate the chemical shifts of the heteronuclei to the chemical shift of nearby protons using dipolar coupling-driven magnetization transfer. The HETCOR method has a clear advantage when more than one proton is attached to the heteronuclear spin of interest or if the proton shifts are of interest. Recently, several pulse sequences for the HECTOR method have been developed. These pulse sequences significantly improve resolution of the proton dimension,[14−17] and they have been applied to some biological systems.[18,19] One of the examples is rotor-synchronized WIM sequences[20] which allow transfer over longer distances. This was demonstrated in $^{31}P-^{1}H$ 2D spectra of bone. Clearly the 1D versions of WIM would not provide quantitative distance information of interest for longer range C−H or N−H pairs, since the long-range distances are often obscured by stronger (but more trivial) hydrogen correlations such as directly bound protons. Thus, the 2D HETCOR method has a unique advantage in studying hydrogen bonding in particular.

2D HETCOR experiments have substantial advantages compared to 1D heteronuclear measurements when information

[†] Department of Chemistry.
[‡] Otsuka Electronics, Inc.
[§] Present Address: Suntory Institute for Bioorganic Research, 1-1-1 Wakayamadai, Shimamoto-cho, Mishima-gun, Osaka 618, Japan.
[⊗] Abstract published in *Advance ACS Abstracts,* December 1, 1995.

(1) Smith, S. O.; Griffin, R. G. *Ann. Rev. Phys. Chem.* **1988**, *39*, 511−535.
(2) McDermott, A.; Gu, Z. In *Encyclopedia of Nuclear Magnetic Resonance;* Grant, D. M., Harris, R. K., Eds.; John Wiley and Sons: New York, 1995 in press.
(3) McDermott, A. E.; Creuzet, F. J.; Griffin, R. G.; Zawadzke, L.; Ye, Q; Walsh, C *Biochemistry* **1990**, *29*, 5767−5775.
(4) Zysmilich, M; McDermott, Ann *J. A. Chem. Soc.* **1994**, *116*, 8362−8363.
(5) Gerstein, B. C.; Pembleton, R. G.; Wilson, R. C.; Ryan, L. M. *J. Chem. Phys.* **1977**, *66*, 361−362.
(6) Gerstein, B. C. *Philos. Trans. R. Soc. London, Ser. A* **1981**, *299*, 521.
(7) Burum, D. P.; Rhim, W. K. *J. Chem. Phys.* **1979**, *71*, 944−956.
(8) Yesinowski, J.; Eckart, H.; Rossman, G. *J. Am. Chem. Soc.* **1988**, *110*, 1367.
(9) McDermott, A. E.; Creuzet, F. J.; Kolbert, A. C.; Griffin, R. G. *J. Magn. Reson.* **1992**, *98*, 408−413.
(10) Munowitz, M. G.; Griffin, R. G. *J. Chem. Phys.* **1982**, *76*, 2848.
(11) Burum, D. P.; Linder, M.; Ernst, R. R. *J. Magn. Reson.* **1981**, *44*, 173−188.
(12) Caravatti, P.; Bodenhausen, G.; Ernst, R. R. *Chem. Phys. Lett.* **1982**, *89*, 363−367.
(13) Caravatti, P.; Braunschweiler, L.; Ernst, R. R. *Chem. Phys. Lett.* **1983**, *100*, 305−310.
(14) Roberts, J. E.; Vega, S.; Griffin, R. G. *J. Am. Chem. Soc.* **1984**, *106*, 2506−2512.
(15) Burum, D. P. *Concepts Magn. Reson.* **1990**, *2*, 213.
(16) Burum, D. P.; Bielecki, A. *J. Magn. Reson.* **1991**, *94*, 645−652.
(17) Bronnimann, C. E.; Ridenour, C. F.; Kinney, D. R.; Maciel, G. E. *J. Magn. Reson.* **1992**, *97*, 522−534.
(18) Lee, C. W. B.; Griffin, R. G. *Biophys. J.* **1989**, *55*, 355−358.
(19) McDermott, A.; Ridenour, C. F. In *Encyclopedia of Nuclear Magnetic Resonance*; Grant, D. M., Harris, R. K., Eds.; John Wiley and Sons: New York, 1995; in press.
(20) Santos, R. A.; Wind, R. A.; Bronnimann, C. E. *J. Magn. Reson.* **1994**, **105B**, 183−187.

0002-7863/96/1518-0822$12.00/0

about hydrogen bonding is desired. Although some information about hydrogen bonding can be derived from the heteronuclear NMR spectra, the information available from the proton shifts is often independent from that obtained from the heteronuclear shifts. One specific example is carboxylic acids: proton shift depends on the interactions of the proton with any nearby hydrogen bond acceptors,[19,21−23] while σ_{22} of ^{13}C shift depends on the hydrogen bonding interactions involving carboxyl oxygen and other nearby protons.[24,25] In the case of the carboxylic anion, the effects of hydrogen bonding on the carbon spectra are pronounced only if the proton is in the so-called "syn" position; carbon shift is rather insensitive to the protons in the "anti" position. The shift of the nearby proton is sensitive to the interaction regardless of the geometry (Gu and McDermott, unpublished results). Therefore, correlated carbon and proton shifts provide much more information about the geometry and strength of the hydrogen bond than either proton or carbon shift alone. HETCOR spectra are useful for assignment of carbon spectra and identification of the chemical nature of the hydrogen bonding partner. The WIM transfer and rotor synchronized WIM sequence can transfer magnetization within C−H pairs separated by as much as 3 Å, which is long enough to cover the range of most hydrogen bonding distances.[17,20] Here we focus particularly on C═O···H−N, C(O)-O-H···O=C type hydrogen bonding partners.

Materials and Methods

Amino acids and dipeptides were purchased from Sigma and used without further recrystallization. Hydrochloride salts were prepared by recrystallization from aqueous HCl solution.

^{13}C CP-MAS spectra were obtained on a Chemagnetics CMX400 spectrometer operating at 99.71 MHz for ^{13}C and 396.5 MHz for ^{1}H. A standard cross polarization pulse sequence with standard phase cycling and background suppression was used; contact time was 3 ms, a 3.5 μs 90° pulse for proton and acquisition times of 25 ms. All carbon spectra were recorded at room temperature and referenced using adamantane (run separately), setting the deshielded peak to 38.6 ppm.

The pulse sequence that we used for the 2D HETCOR experiment is shown in Figure 1[16,17] with rotor-synchronization sometimes employed.[20] In this pulse sequence, the spin system was prepared by a single 90° pulse, followed by proton chemical shift evolution period, while $^{1}H-^{1}H$ dipolar interaction was eliminated by BLEW-24 and $^{13}C-^{1}H$ heteronuclear dipolar coupling eliminated by ^{13}C BB-24 decoupling. Afterwards, WIM-24 was used to transfer polarization selectively from the protons to the carbon spins via heteronuclear dipolar interaction with homonuclear coupling suppressed. WIM-24 pulse sequence should be used for less than half a rotor cycle for maximum transfer efficiency. For the rotor-synchronized HETCOR pulse sequence, the signal was added over several rotor periods in order to obtain longer range couplings; thus, the number of WIM-24 cycles was variable.[20] Typical cross polarization times were about 130 μs for spectra reported in this paper, and the effect of the length of the cross polarization time will be discussed later. Finally, the ^{13}C FID was detected during ^{1}H decoupling. TPPI phase sensitive detection scheme was used to obtain pure phase 2D spectra.[26,27] 2D $^{1}H-^{13}C$ HETCOR experiments were performed at both 200 and 400 MHz, and these spectra are compared in the text. HETCOR spectra employed 48, 64, or 80 points in the t_1 period (^{1}H dimension) and were zero filled to 512 points. In the t_2 period (^{13}C dimension), 300 or 512 points were taken and zero filled to 1024 points. When the TPPI phase sensitive detection scheme was used for the t_1 detection, the proton carrier frequency was shifted about 1−2 kHz to avoid phase twist artifacts at the carrier frequency. ^{1}H and ^{13}C 90° pulse times ranged from 3.2 to 3.4 μs and were matched within 0.1 μs. MAS speed was between 1.5 and 3.0 kHz. The recycle delay was between 2 and 10 s, and 48−600 scans were accumulated. Approximately 100 mg of each sample was used. Total experiment time varied from 4 to 12 h. Spectra were processed using FELIX (Biosym); level multipliers were set geometrically with a multiplier of between 1.5 and 2.0 to optimize the presentation.

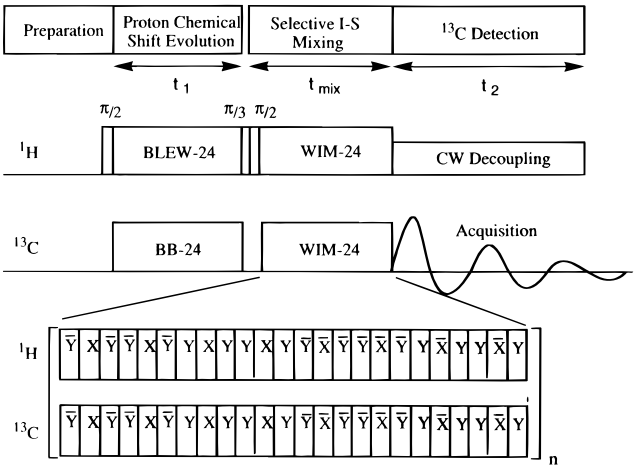

Figure 1. Schematic diagram of the pulse sequence of the 2D $^{1}H-^{13}C$ HETCOR experiment. For discussion of the sequence see the Materials and Methods and refs 11−17, 20. As explained in text, half cycles of the sequences (Wim-12 or BLEW-12) were used in certain cases.

Results and Discussion

Magnetization Transfer Rates using the WIM Cross Polarization Sequence. In order to characterize the rates of cross polarization using the WIM-24 transfer pulse sequence, several studies were performed in which carbons were polarized from the protons using WIM and 1-D carbon spectra were recorded as a function of the transfer time ("build-up curves"). These studies help to ascertain whether spin diffusion among the protons is significant during the cross polarization time. In the absence of proton spin diffusion the accumulated transfer or the carbon intensity should build up at the beginning of each rotor cycle, maximize at the middle of the rotor cycle and decay back to zero at the end of each rotor cycle. This point is discussed in more detail below.

Figure 2 shows a series of WIM24 "build-up" curves for various carbons in Ala-Asp and in glycine. In this experiment, one rotor cycle contains 10 WIM-24 half-cycles. The carbon intensities for carboxyl and carbonyl groups increase monotonically through the first half of the rotor period and then monotonically decay through the second half of the rotor period. Furthermore, this behavior is repeated during the second rotor cycle. This oscillation suggests that proton spin diffusion is not rapid on the time scale of the HETCOR experiment, and therefore, this method might be useful for approximate distance measurements.

The "build-up" curves for the CH and CH_2 groups are rather different from those of the carboxy groups; they both increase rapidly at the beginning of the rotor cycle, reach a plateau, and then the C−H groups maintain carbon intensity until near the end of the rotor cycle, while the CH_2 groups decrease gradually throughout the rotor period. Both groups show another increase in signal intensity at the beginning of the second rotor cycle. The rise time of the carbon intensity is determined mainly by

(21) Bhat, T. N.; Vijayan, M. *Acta Crystallogr. B* **1976**, *32*, 891−895.
(22) Berglund, B.; Vaughan, R. W. *J. Chem. Phys.* **1980**, *73*, 2037−2043.
(23) Harris, R. K.; Jackson, P.; Merwin, L. H.; Say, B. J.; Hagele, G. *J. Chem. Soc., Faraday Trans. 1* **1988**, *84*, 3649−3672.
(24) Gu, Z.; McDermott, A. *J. Am. Chem. Soc.* **1993**, *115*, 4282−4285.
(25) Gu, Z.; Zambrano, R; McDermott, A. *J. Am. Chem. Soc.* **1994**, *116*, 6368−6372.
(26) Drobny, G.; Pine, A.; Sinton, S.; Weitekamp, D. P.; Wemmer, D. *Faraday Symp. Chem. Soc.* **1979**, *13*, 49−55.
(27) Kessler, H.; Gehrke, M.; Griesinger, C. *Angew. Chem., Int. Ed. Engl.* **1988**, *27*, 490−536.

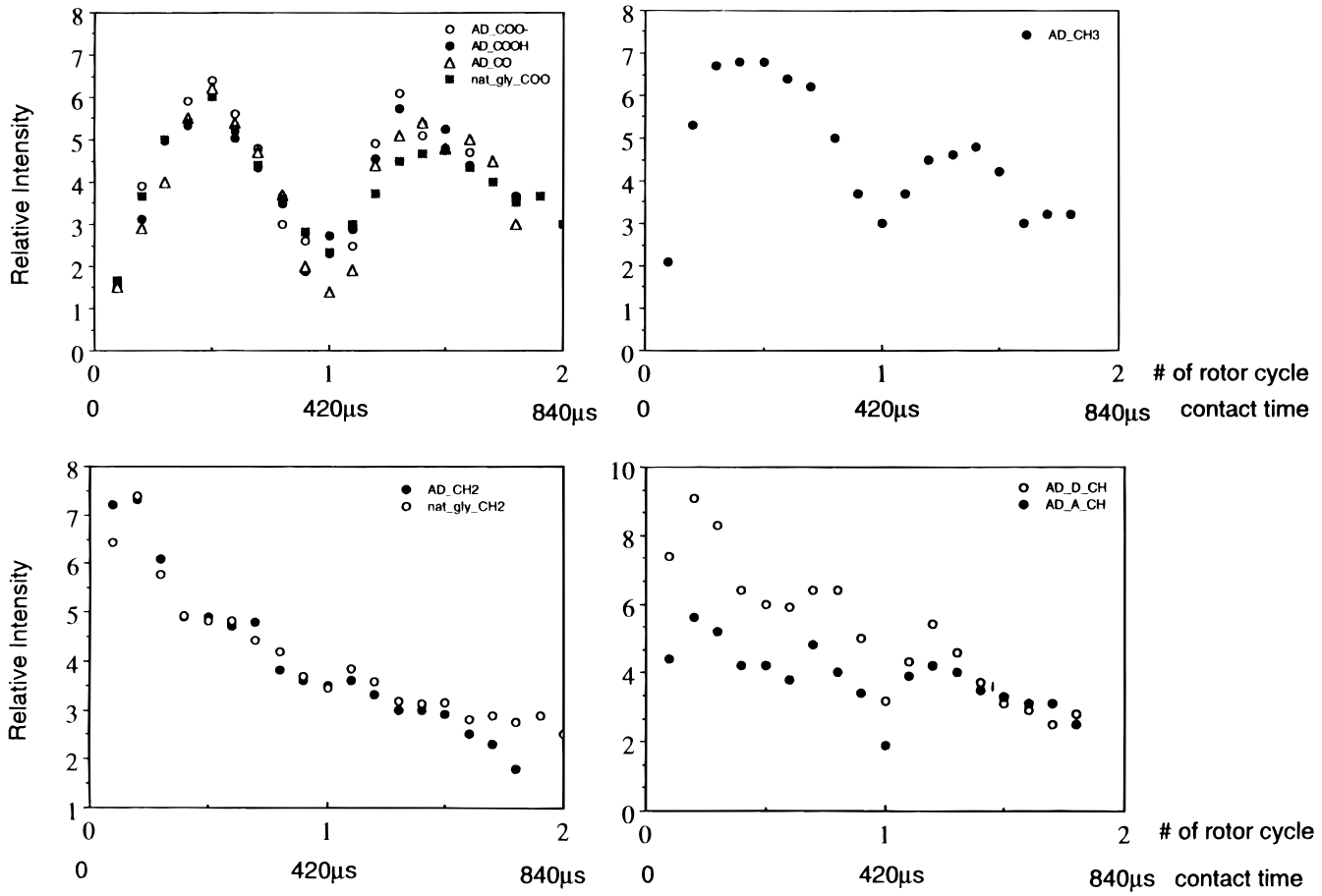

Figure 2. Carbon intensities of the indicated resonances of glycine and Ala-Asp during a WIM cross polarization experiment. The abscissa indicates the length of the WIM cross polarization time, shown both in microseconds and in rotor periods. Each large tic represents a rotor period or 10 WIM-24 half cycles. A data point was taken after each WIM half-cycle. Note that for directly bound proton carbon pairs the polarization transfer is nearly saturated after a single WIM half-cycle, while for long-range (2.5−3 Å) correlations the polarization continues to build up during the first half of the rotor period. Note also that the magnetization decays in all cases near the end of the rotor cycle because, under the influence of the homonuclear decoupling, the heteronuclear coupling averages to zero after a full rotor cycle. Upper left panel shows all carboxyl carbons (○, the carboxylate of Ala-Asp; ●, the neutral carboxylic acid in Ala-Asp, △, is the amide carbonyl in Ala-Asp; ■, the carboxylate group of glycine. Upper right panel represents the data from the methyl group of Ala-Asp. Lower left panel represents the methylene groups of Ala-Asp (●) and glycine (○). Lower right panel represents the data for the two methyne groups of Ala-Asp.

the strength of the C−H dipolar coupling, which is about 30 kHz for the directly bound pairs and 1 kHz for the a C−H pair in a hydrogen bonded arrangement such as C═O···H−X. For the directly bound pairs the transfer is rapid enough that the carbon magnetization is essentially saturated within a single WIM half-cycle (roughly 30 μs). A detailed description of the behaviors of isolated CH, CH_2, and CH_3 spin systems during the WIM24 sequence has been published by Burum et al.[28] In contrast, weak coupling for C−H pairs with distances in the range 2−3 Å leads to a monotonic and slow WIM "build-up" during the first part of the rotor cycle. The peak volume of the direct bound C−H spin pair is not an ideal reference for calibrating the distance measurements. However, because the distances are essentially invariant and these pairs are present in all of the spectra, we nevertheless have decided to use them for reference volumes. The saturation in the reference peak is probably the main cause of scatter in the correlation between HETCOR peak volume and distance, which is plotted in Figure 8 and discussed later in the text.

Assignment and Hydrogen Bonding Partner Identification. Figure 3 gives the 400 MHz HETCOR spectrum of natural abundance valine hydrochloride as a simple example, along with the corresponding 1D ^{1}H and ^{13}C projections of the spectrum displayed along the appropriate axis; valine hydrochloride is a particularly simple case and was selected, because it does not have strong intermolecular hydrogen bonding or correlations, and only intramolecular correlations would show up.[29] For this sample the longest dipolar transfer involves a distance of 2.7

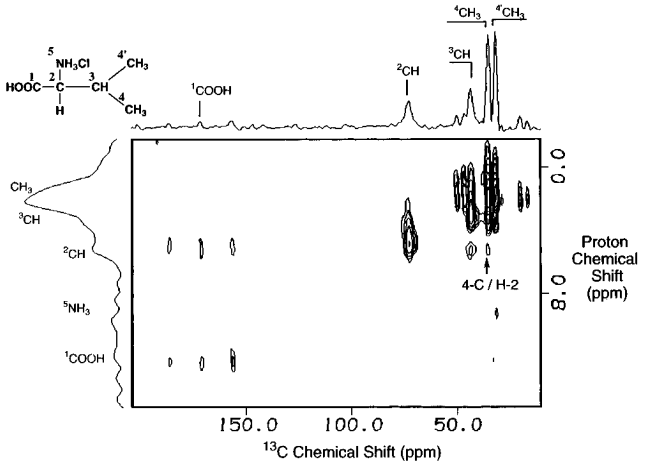

Figure 3. 2D HETCOR spectrum of valine hydrochloride measured at 400 MHz. The top trace is the projection of the carbon spectrum and the left is the ^{1}H projection. The assignments of the lines are indicated on the two 1D projections. The spectrum was acquired using 48 t_1 points, 512 t_2 points, and two WIM-rotor cycles.

(28) Burum, D. P.; Blelecki, A. *J. Magn. Reson.* **1991**, *95*, 184−190.

Å. All of the cross peaks involving amine protons are missing; the absence of these peaks presumably results from motion of the NH_3^+ group which will be discussed later in this paper. The assignment of two methyl peaks in the carbon spectrum has been a long-standing problem. However, by using the HETCOR spectrum, the 4 and 4′ carbons of two methyl groups can be assigned very clearly according to the cross peaks to the H-2 proton. The neutron data show that the distance between 4-C and H-2 is 2.67 Å and that between 4′-C and H-2 is 3.48 Å. The HETCOR spectrum clearly shows only one cross peak (labeled as 4-C/H-2) in the region of the methyl carbon and α-proton (H-2). Thus, the shielded methyl peak is from the 4′ carbon and the deshielded carbon peak is the 4 position methyl. This case illustrates an enormous potential for HETCOR in assigning complicated 1D spectra. This observation also strongly supports our assertion that homonuclear spin-diffusion during the HETCOR experiment is not particularly rapid, since one would expect to see both cross peaks if there is extensive spin diffusion. Other cross peaks from spin pairs involving C−H distances above 3 Å are similarly missing, for example, 1-C/H-3, 1-C/H-4,4′, 2-C/H-4,4′, and 4,4′-C/H-1.

Figure 4a shows the 400 MHz spectrum of natural abundance Ala-Asp dipeptide. The three carbonyl-type carbons are easily assigned by virtue of their different ^{13}C CSA values,[25] with one being a protonated carboxyl (isotropic shift at 174 ppm), another one being a deprotonated carboxylate (178 ppm) and the third being a carbonyl group (172 ppm). The aliphatic group region can also be unambiguously assigned by the chemical shifts as marked in the 1D projection.

As indicated by the X-ray crystal structure,[30] there are several strong hydrogen bonds in this compound. The strongest one is between the proton of the protonated carboxyl and the oxygen of the deprotonated carboxyl, with an O···O distance of 2.609 Å and a H···O distance of 1.69 Å. The corresponding H···C distance is 2.5 Å. In the region of the HETCOR spectrum in which ^{13}C signals of carbonyls correlate with deshielded proton shifts characteristic of acids, there are two sets of cross peaks: one is from the carbon of the (neutral or protonated) carboxylic acid to the proton of the same carboxylic acid, which is very intense, and the other cross peak is from the carbon of the deprotonated carboxyl group to the acidic proton, which is weak but noteworthy since it arises from intermolecular hydrogen bonding.

Additional intramolecular cross peaks can greatly help the assignment of both ^{13}C and ^1H. For example, from ^1H NMR alone, the assignments of the −NH and $-NH_3^+$ proton peaks are ambiguous. However, only one assignment can account for the cross peaks from the protons in these groups. The amide proton is correlated with the carbon of the aspartic methyne group (which is relatively deshielded) while the amine proton is correlated to the carbon of the alanyl methyne (which is relatively shielded) (please refer to Figure 4a, expansion I). Additional evidence comes from the fact that the amide proton resonance exhibits the expected cross peak to the nearby carbonyl C═O (Figure 4a, expansion II). Furthermore, assignment of carbons 1, 4, and 8 is verified by comparing the proton cross peaks in the carbonyl resonance to those in the aliphatic region. In addition, the protonated acid carboxyl (C-8) is correlated to the CH_2 protons, while carbons 1 and 4 both show correlations to the methyl protons (please refer to Figure 4a, expansion II).

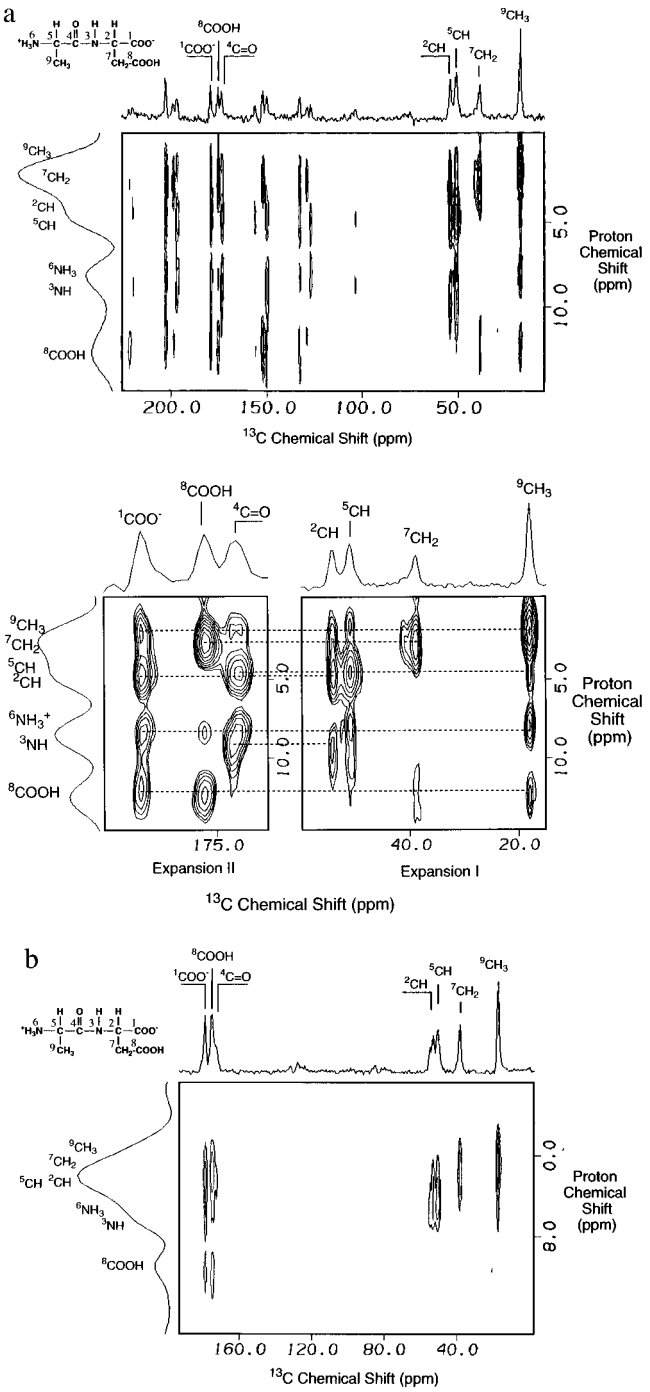

Figure 4. (a)2D HETCOR spectrum of the Ala-Asp measured at 400 MHz. The top is the projection of the carbon spectrum and the left shows the ^1H projection. The proposed assignments were indicated on the two 1D spectra. The spectrum was acquired using 48 t_1 points, 512 t_2 points, three half-WIM cycles per rotor cycle, and two rotor cycles, and the spectral width is 33.3 kHz. Below we show expansions I and II from (a). Lines are included as a guide for the assignments. (b) 2D HETCOR spectrum of the Ala-Asp measured at 200 MHz measured using the rotor synchronized HETCOR sequence. The top is the projection of the carbon spectrum and the left shows the ^1H projection. The assignment is indicated on the two 1D projections. The spectrum was acquired using 64 t_1 points, 300 t_2 points, four half-WIM cycles per rotor cycle, and three rotor cycles.

On the other hand, cross peaks due to correlations for spin pairs with C−H distances larger than 3 Å are clearly missing in the spectra, such as, for example, the 2-C/H-7, 4-C/H-8, 5-C/H-8, 2-C/H-8, and 7-C/H-6 spin pairs. These results clearly show that homonuclear spin diffusion is not rapid during this experiment. It is also noted that several cross peaks are

(29) Koetzle, T. F.; Golic, L.; Lehmann, M. S.; Verbist, J. J.; Hamilton, W. C. *J. Chem. Phys.* **1974**; *60*, 4690−4696.

(30) Eggleston, D. S.; Hodgson, D. J. *Int. J. Peptide Protein Res.* **1983**, *21*, 288−295.

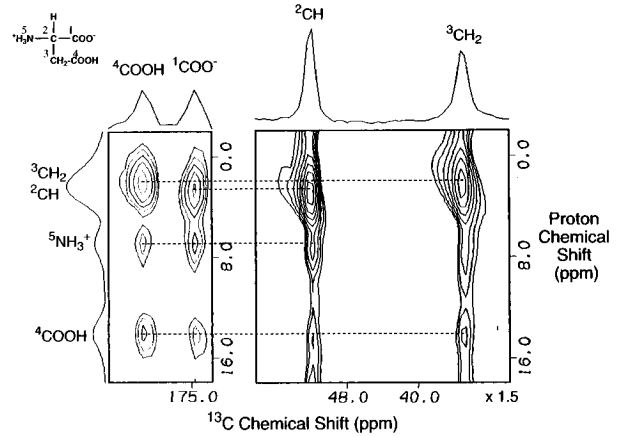

Figure 5. Expansion plot of 2D HETCOR spectrum of the DL-aspartic acid measured at 400 MHz. The top is the projection of the carbon spectrum, and the left shows the ^{1}H projection. The assignments were marked on the 1D spectra. The spectrum was acquired using 40 t_1 points, 512 t_2 points, and three half-WIM cycles per rotor cycle, and the spectral width is 33.3 kHz. The contour levels of the right panel are 1.5 times of those in the left panel for the purpose of clear presentation. Lines are included as a guide for the assignments.

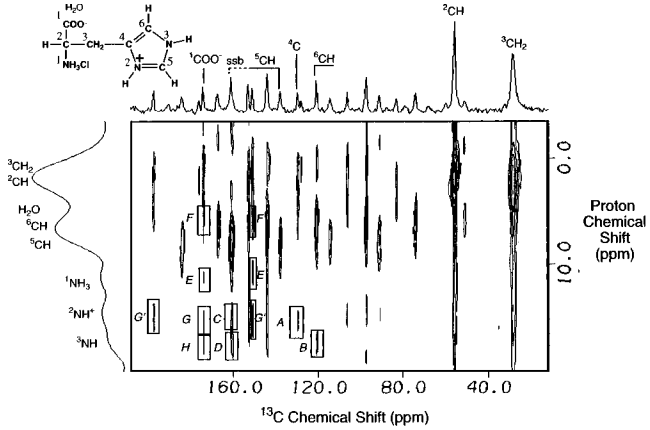

Figure 6. 2D HETCOR spectrum of histidine monohydrochloride monohydrate measured at 400 MHz. The top trace is the projection of the carbon spectrum, and at the left is the projection of the proton spectrum. The assignments of the peaks are indicated on the two 1D projections. The spectrum was acquired using 48 t_1 points, 512 t_2 points, and two WIM-rotor cycles. The letter labels for the cross peaks are listed as follows (A) 4-C/H(2-N); (B) 6-C/H(3-N); (C) 5-C/H(2-N); (D) 5-C/H(3-N); (E): 1-C/H(1-N); (F) 1-C/H(H_2O); (G) 1-C/H(2-N); (H) 1-C/H(3-N).

apparently missing, although they should appear in the spectrum. This phenomena is largely due to overlap with stronger neighbor cross peaks, such as the case of 2-C/H-7, which is obscured by the much stronger 2-C/H-2 cross peak, and 2-C/H-7 appears as a tail of the larger neighboring peak.

Figure 5 shows an expansion plot of the HETCOR spectrum of DL-aspartic acid, which again illustrates the utility of the spectrum for peak assignments. Normally, the carbon shifts for deprotonated carboxyl groups are deshielded relative to the neutral acids, but a strong cross peak from the deshielded carbon to the acidic proton in the HETCOR spectrum unambiguously indicates that the opposite is the case for the two groups in this particular molecule. A weak cross peak from the shielded carbon to the acidic proton is due to intermolecular hydrogen bonding with a distance of 2.5 Å.[31] Assignments for the carbons based upon HETCOR data are consistent with those based upon the carbon CSA.

Histidine hydrochloride monohydrate exhibits interesting and rather strong hydrogen bonds involving the imino protons N−H interacting with carboxylates, water interacting with the carboxylate group, and an amine also interacting with carboxylate groups.[32,33] The HETCOR spectrum of this compound is shown in Figure 6, with the assignments indicated along the corresponding projections. The assignment of the carbon spectrum is based on the previous SSNMR and solution NMR data.[25,34] The assignment of the proton spectrum is based on the cross peak correlations in the HETCOR spectrum. The H(2-N) and H(3-N) can be assigned without any ambiguity, since H(2-N) is next to 4-C and H(3-N) is next to 6-C, so the cross peak labeled A arises from an H(2-N) correlation and the cross peak labeled B arises from an H(3-N) correlation. Furthermore, both H(2-N) and H(3-N) have strong cross peaks labeled C and D to 5-C although they are apparently visible as one overlapped peak on the spinning sideband of 5-C. The H(1-N) of the amine group can be assigned through the cross peaks labeled E. This assignment is same as a previously reported assignment for the CRAMPS spectrum of the histidine monohydrochloride monohydrate.[35] The only peak which has some degree of ambiguity is that of water since it is not resolved in our spectrum. Since the intensities of amine and water proton regions are largely dependent on the motion of those groups, we are currently measuring temperature-dependent 2D HETCOR experiment. However, those ambiguities did not affect the assignment of this compound.

Hydrogen bonding between the water and the carboxylate group, as well as both the imines and the carboxylates, is expected to be seen in the HETCOR plot. These peaks are indicated in Figure 6, as cross peaks F, G, and H. These peaks are not especially well resolved; however, they appear as expected. The water proton peak is located between the imidazole proton and aliphatic proton peaks. Cross peak G (H(2-N) interacting with 1-COO^-) together with cross peaks G′ (the spinning sidebands of cross peak G) are much more intense than cross peak H (H(3-N) interacting with 1-COO^-), which is consistent with the neutron crystal data in that the C−H distance of the H(2-N)···O═C is 2.5 Å while that of the H(3-N)···O═C is 2.9 Å, i.e., 0.4 Å longer. This spectrum also lacks cross peaks between spin pairs with C−H distances above 3 Å. For example, 5-C/H(2-C), 5-C/H(3-C), and 4-C/H(5-C) correlations were not observed.

Effect of Pulse Lengths, Motion, and Applied Field Strength: Discussion of Possible Proton Spin Diffusion Effects in the Correlation Spectra. In HETCOR spectra, the interpretation of the proton dimension is subject to similar complications as are CRAMPS spectra. For example, a well-resolved spectrum requires carefully adjusted pulse lengths. In addition, the intensities of certain functional groups depend strongly on the presence or absence of motions on the microsecond time scale, which can be independently investigated by temperature-dependent, static deuterium line shape methods.[19,36] A recent publication discusses this problem extensively.[37] Motions on the mid-kilohertz time scale ($\tau_c \sim 10^{-4}$ s) will affect the line shape in a way that will explicitly depend upon the correlation time for the motion and on the pulse

(31) Rao, S. T. *Acta Crystallogr. B* **1973,** *29*, 1718−1720.
(32) Fuess, H.; Hohlwein, D.; Mason, S. A. *Acta Crystallogr. B* **1977**, *33*, 654−659.
(33) Hohlwein, D. *Acta Crystallogr. A* **1977**, *33*, 649−654.
(34) Ye, C.; Fu, R.; Hu, J.; Ding, S. *Magn. Reson. Chem.* **1993**, *31*, 699−704.
(35) Naito, A.; Root, A.; McDowell, C. A. *J. Phys. Chem.* **1991**, *95*, 3578−3581.
(36) Gu, Z.; McDermott, A. Manuscript in preparation.
(37) Long, J. R.; Sun, B. Q.; Bowen, A.; Griffin, R. G. *J. Am. Chem. Soc.* **1994**, *116*, 11950−6.

lengths. Amine functional group as well as water molecules often display hopping motions on this time scale at room temperature. In practice, we have observed a pronounced difference between the amine peak intensities with probe performance and characteristic pulse lengths.

Curiously, in some HETCOR spectra we have also observed dramatic differences in the intensities of amine cross peaks when we compare spectra taken at 200 and 400 MHz, even if the pulse lengths were similar. Figure 4b shows the 2D HETCOR spectrum of Ala-Asp measured at 200 MHz with $t_{90}^{\circ} = 3.2$ μs. Cross peaks in the amine region are missing in the 200 MHz spectrum although they are detectable at 400 MHz. This striking difference was surprising since the pulse lengths were not very different. We expected higher sensitivity at 400 MHz magnetic field, but we observed a very modest improvement. The HETCOR pulse sequence requires a spinning speed of about 2 kHz, so as expected, more spinning side bands are observed which sometimes complicates assignment but can offer interesting geometrical information about hydrogen bonding networks. The carbonyl and aromatic regions were indeed very crowded at 400 MHz. Long-range couplings (2.6−3.0 Å) were often far more apparent in the 400 MHz spectra than in the 200 MHz spectra, especially those involving amine groups, even though the pulse lengths were not very much different.

It is important to discuss whether the long range cross peaks (with C−H distances of 2.6−3.0 Å) in the 400 MHz spectrum could arise from processes involving proton spin diffusion. The cross peaks observed in the 400 MHz spectrum are all associated with C−H pairs with distances of less than 3.0 Å, and we observe the expected decrease in peak volume with increasing distance. These facts indicate that random spin diffusion is not the main reason for these additional peaks in the 400 MHz spectrum. Spectra of carbon-13 enriched glycine cocrystallized with deuterated glycine also showed intensity patterns similar to the natural abundance material, indicating that long-range spin diffusion does not play an important role in the 400 MHz experiment (data not shown). The WIM-24 buildup curves measured for Ala-Asp at 400 MHz showed that the carbon signal disappeared when the number of WIM24 cycles was set to a full rotor period, which would indicate that the proton spin diffusion is not significant. Deliberately mis-set pulse lengths for the proton did not appear to bring in additional cross peaks, but rather resulted in severe broadening of the proton dimension. A series of experiments were attempted in which we mis-set the proton pulse lengths. Spectra of Ala-Asp and histidine hydrochloride monohydrate were measured, and if the pulse length was in error by about 0.05 μs the spectra were of reasonable quality but the signal-to-noise ratios and the proton resolution became noticeably worse when the pulse length error reached 0.2 μs.

Since low spinning speeds are used for the HETCOR experiment, anisotropic groups such as carbonyls and aromatic groups give rise to a large set of spinning side bands. For many of the compounds, the intensities among the spinning side bands corresponding to a given carbon are not those expected from its static tensor or from CP-MAS data. Figure 7 shows the CPMAS spectrum of the CO_2H group from valine hydrochloride compound compared with its HETCOR slices from the α and the acid hydrogens. The spinning side bands from the acid proton correlation are clearly different from the CPMAS pattern. This distortion in the intensities of the side bands is typical for the asymmetric groups and is a result of the correlation of the dipolar axis with particular elements of the CSA tensor axes. For the protonated carboxylic acids the geometry of the CSA axes and of the proton axes relative to the carbon ones is fixed,

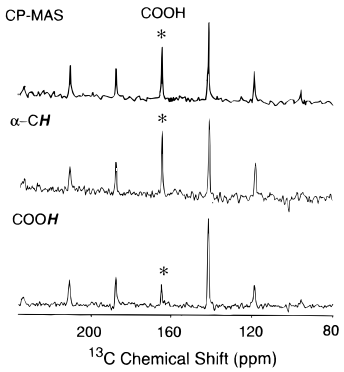

Figure 7. CP-MASS spectrum of valine hydrochloride is compared with the ^{13}C HETCOR carbon slices corresponding to correlations with the α and acidic protons. Clear distortions in the spinning sideband intensities may be seen for HETCOR slices, which presumably reflect the relative orientations of the dipolar axes and the carbon CSA axes.

and as a result the distortion of the carbon CSA in the correlation with the acid proton gives a specific reproducible pattern in which the region near the centerband is particularly weak. This results directly from the fact that the proton carbon dipolar axis is nearly coincident with the least shielded tensor axis.

C−H Distance Estimates. Cross peaks for directly bonded carbon and proton pairs and for indirectly bonded carbons and protons pairs for Ala-Asp and histidine hydrochloride have volumes that scale inversely with the dipolar coupling. Therefore, we attempted to correlate the intensities of cross peaks to the C···H distances for our whole database of compounds. The rate of dipolar transfer, or cross peak "build-up rate", would yield much more accurate distances than a single peak volume at a particular mixing time. For this study, we have only considered peak volumes for a single short mixing time (∼130 μs) because of practical limitations.

The 2D HETCOR experiment for an I and S spin system involves dipolar interaction whose Hamiltonian can be expressed as

$$H_{IS} = ID_{IS}S = \gamma_I\gamma_S h r_{IS}^{-3} f(\theta,\psi)$$

where D is dipolar coupling and $f(\theta,\psi)$ describes the dipolar orientation relative to the static field and is time dependent during magic angle spinning.[38,39] During the WIM-24 pulse sequence (unlike the usual Hartman−Hahn cross-polarization sequence) the C−H dipolar Hamiltonian is analogous to an inhomogeneous heteronuclear coupling in that the multiple pulse train decouples proton homonuclear interactions. As a result, heteronuclear dipolar coupling varies during the rotor cycle so as to refocus all dipolar evolution and average the coupling to zero after each full rotor cycle. As a result, the transfer can be very efficient within any spin pair for approximately half of a rotor cycle, but for a complete rotor cycle the time-averaged coupling is zero, the effects of the dipolar coupling are refocused, and the transfer is poor. For short contact times, a monotonic relation between the coupling strength (or $1/r^3$) and the magnetization transfer rate (or the peak volume) could be expected as long as molecular motion and multiple couplings are ignored. (This is in contrast with the NOE as used in liquid state NMR, where the transfer is driven by fluctuations in the average dipole, so the magnetization transfer rates depend on $1/r^6$.) Thus, HETCOR peak volumes could serve as a useful

(38) Mehring, M. *High Resolution NMR Spectroscopy in Solids*, 2nd ed.; Springer: Berlin, 1983.

(39) Ernst, R. R.; Bodenhausen, G.; Wokaun, A. *Principles of Nuclear Magnetic Resonance in One and Two Dimensions*; Oxford: New York, 1992.

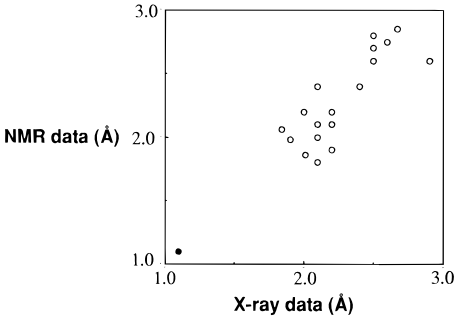

Figure 8. Plot of the correlation between C−H distance as measured by neutron diffraction or X-ray analysis and that estimated from the HETCOR peak volumes. A distance was estimated from each peak volume by calibration with a directly bound C−H correlation involving the same proton and assuming that the volume is proportional to the inverse cube of the distance. The distance estimates agreed with the crystallographic distance within standard deviation of 0.2 Å in general. Peaks involving mobile protons have been excluded.

structural probe, but significant complications to this simple rule should be expected. To improve the situation for very weak couplings, the rotor-synchronized WIM transfer sequence involves C−H contact for the "first half" of every cycle during several rotor periods, so the average C−H dipolar coupling is not zero and transfer over longer periods of time and over longer distances is possible.

Several sources of error in estimating distances using the cross peak volumes should be anticipated. First, our reference peaks involve couplings so strong that the transfer is nearly saturated within one WIM half cycle, as discussed above. To compare intensities of cross peaks involving different protons, we need to consider the effects of motion of the protons, as discussed above, and we are unable to do any quantitative estimations at the moment. Furthermore, the efficiency of magnetization transfer could depend on whether the C−H system is effectively an A−X an $A-X_2$, or an $A-X_3$.[28] Such a difference is indicated by the dramatic changes in the WIM build-up curves (Figure 2). In small molecule studies some peaks include contributions from both intermolecular and intramolecular correlations. Thus, it is not evident that a simple accurate relation between distance and peak volume will emerge.

Nonetheless, we examined the relation between peak volume (for which we used the sum of all the spinning side bands) and internuclear distance for our database of compounds. The covalent C−H bond length which is generally 1.07−1.09 Å serves as an internal standard for most cases. We have calibrated cross peaks for each proton using a cross peak involving a known intramolecular distance and estimated the distances from that proton to other carbons assuming that the peak volume is proportional to the inverse cube of the distance. With the exception of mobile groups such as methyl groups, the peak volumes did correlate well with $1/r^3$, and we concluded that distances could be estimated in this fashion to with standard deviation of 0.2 Å (Figure 8), while the largest difference is 0.3 Å, which could be quite useful in structural studies. The data for each individual compound are discussed below.

Figure 9 shows the HETCOR spectrum of the [$^{13}C_2$-1,2]-glycine. From the published neutron diffraction structure,[40] this compound has only four intramolecular C···H correlations: the amine proton to 2-C (2.09 Å), the amine protons to 1-C (2.6, 3.1, 3.2 Å), the H-2 to 1-C (2.15 Å), and the directly bonded H-2 proton to 2-C (1.09 Å). The intermolecular hydrogen correlation (amine protons to 1-C) (2.5, 2.8, 2.9, 3.4 Å) is

(40) Power, L. F.; Turner, K. E.; Moore, F. H. *Acta Crystallogr. B* **1976**, *32*, 11−16.

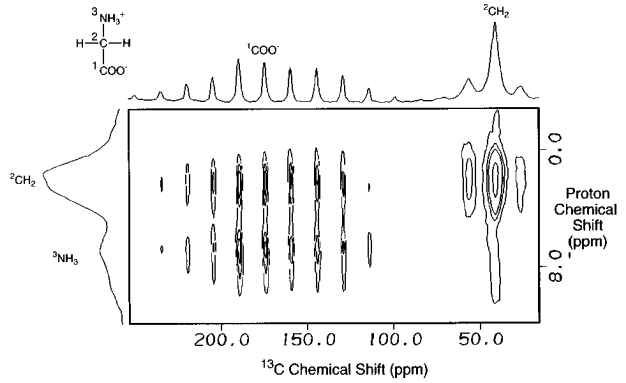

Figure 9. 2D HETCOR spectrum of the 1,2-^{13}C glycine measured at 400 MHz. The top trace is the projection of the carbon spectrum, and on the left the ^{1}H projection is shown. The assignments of the peaks are indicated on the two 1D spectra. The spectrum was acquired using 48 t_1 points, 512 t_2 points, and two WIM-rotor cycles.

Table 1. Distance Measurements (Å) from the Glycine HETCOR Spectrum[a]

	1-C/H-2	1-C/H-3	2-C/H-2	2-C/H-3
neutron data	2.15	2.5	1.1	2.1
SSNMR data	*2.15*	2.6	*1.1*	2.4

[a] The distances between carbons and hydrogens determined by X-ray or neutron diffraction are entered and compared with those estimated from HETCOR spectra. The HETCOR distances are calculated by assuming that the cross peak volumes are proportional to $1/r^3$ and using a cross peak associated with a covalent C−H bond as a calibration value. The data agree within 0.3 Å except where extensive motion of the protons is involved. The ‡ symbol (Tables 3−5) represents an intermolecular interaction.

Table 2. Distance Measurements (Å) from Valine·HCl HETCOR Spectrum[a]

	1-C/H-2	1-C/H-1	3-C/H-3	3-C/H-2
Neutron data	2.15	1.90	1.09	1.84
SSNMR data	*2.15*	1.98	*1.1*	2.06

	4-C/H-4	4-C/H-2
neutron data	1.07	2.67
SSNMR data	*1.07*	2.85

[a] The distances between carbons and hydrogens determined by X-ray or neutron diffraction are entered and compared with those estimated from HETCOR spectra. The HETCOR distances are calculated by assuming that the cross peak volumes are proportional to $1/r^3$ and using a cross peak associated with a covalent C−H bond as a calibration value. The data agree within 0.3 Å except where extensive motion of the protons is involved. The ‡ symbol (Tables 3−5) represents an intermolecular interaction.

difficult to detect because of the analogous intramolecular distance. Using the volumes of the 2-C/H-2 and 1-C/H-2 cross peaks as references, we calculated average distances between 2-C and H-3 and between 1-C and H-3; those are tabulated in Table 1. The cross peak from 1-C to H-3 involves intra- and intermolecular couplings. Since our analysis included only one distance, the distance from 1-C to H-3 calculated on the basis of the peak volume has a systematic bias. The calculated distances along with neutron data from valine hydrochloride are also listed in table2.

Data for DL-aspartic acid are summarized in Table 3 in the form of several distances calculated from the volumes of those cross peaks in the HETCOR spectrum, showing a reasonable correlation between peak volumes and the distances from diffraction data. In this case, the signal from the NH_3^+ is relatively weak, and presumably the motion of this group affects the accuracy of distances for several compounds.

Table 3. Distance Measurements (Å) from DL-Aspartic Acid HETCOR Spectrum[a]

	1-C/H-2	1-C/H-4‡	1-C/H-5	4-C/H-4
X-ray data	2.05	2.60	2.8	1.9
SSNMR data	*2.05*	2.75	4.8	*1.9*
		4-C/H-3		4-C/H-5
X-ray data		2.01		2.8
SSNMR data		1.86		4.7

[a] The distances between carbons and hydrogens determined by X-ray or neutron diffraction are entered and compared with those estimated from HETCOR spectra. The HETCOR distances are calculated by assuming that the cross peak volumes are proportional to $1/r^3$ and using a cross peak associated with a covalent C−H bond as a calibration value. The data agree within 0.3 Å except where extensive motion of the protons is involved. The ‡ symbol (Tables 3−5) represents an intermolecular interaction.

Table 4. Distance Measurements (Å) from Alanylaspartate HETCOR Spectrum[a]

	1-C/H-2	1-C/H-6 ‡	1-C/H-8 ‡	1-C/H-9 ‡
X-ray data	2.1	2.6	2.5	2.8
SSNMR data	*2.1*	3.2	2.7	3.6
	2-C/H-2	2-C/H-3	4-C/H-5	4-C/H-3
X-ray data	1.1	2.1	2.1	2.0
SSNMR data	*1.1*	1.8	*2.1*	2.2
	4-C/H-9	5-C/H-5	5-C/H-3	5-C/H-6
X-ray data	2.7	1.1	2.4	2.1
SSNMR data	3.4	*1.1*	2.4	2.1
	5-C/H-9	8-C/H-8	8-C/H-6	8-C/H-7
X-ray data	2.2	1.9	3.3	2.1
SSNMR data	2.8	*1.9*	3.9	2.0
	9-C/H-9	9-C/H-5	9-C/H-6	9-C/H-8 ‡
X-ray data	1.1	2.2	2.6	3.3
SSNMR data	*1.1*	1.9	2.0	1.7

[a] The distances between carbons and hydrogens determined by X-ray or neutron diffraction are entered and compared with those estimated from HETCOR spectra. The HETCOR distances are calculated by assuming that the cross peak volumes are proportional to $1/r^3$ and using a cross peak associated with a covalent C−H bond as a calibration value. The data agree within 0.3 Å except where extensive motion of the protons is involved. The ‡ symbol (Tables 3−5) represents an intermolecular interaction.

Alanylaspartic acid provides a good example of distance measurements in a relatively complex system. Table 4 lists all the distances that were measured from the HETCOR spectrum of Ala-Asp. Again, we observed a good correlation between a peak volume and a distance except for the distances involving the mobile methyl group. The correlations included several intermolecular C−H distances such as 1-C/H-6, 1-C/H-8, 1-C/H-9, and 9-C/H-8, and they all give a very reasonable agreement except for 9-C/H-8, which involves the methyl carbon.

Table 5 also lists the distances measured from the HETCOR spectrum of histidine hydrochloride monohydrate. The distances measured by NMR give fairly good agreement with crystallography except for that of the water to carboxylate correlations which result from intermolecular hydrogen bonding. It is possible that conformational dynamics of the water molecule are responsible for this discrepancy, and further NMR studies should be performed to verify this hypothesis.

Table 5 Distance Measurements (Å) from Histidine Monohydrochloride Monohydrate HETCOR Spectrum[a]

	1-C/H-2	1-C/HW ‡	1-C/H(1-N)	1-C/H(2-N)
neutron Data	2.1	2.9	2.7	2.5
SSNMR data	*2.1*	3.2	>5	2.8
	4-C/H-3	4-C/H-6	4-C/H(2-N)	6-C/H-6
neutron data	2.1	2.1	2.2	1.1
SSNMR data	*2.1*	2.0	2.1	*1.1*
		6-C/H-3		6-C/H(3-N)
neutron data		2.9		2.2
SSNMR data		2.6		2.2

[a] The distances between carbons and hydrogens determined by X-ray or neutron diffraction are entered and compared with those estimated from HETCOR spectra. The HETCOR distances are calculated by assuming that the cross peak volumes are proportional to $1/r^3$ and using a cross peak associated with a covalent C−H bond as a calibration value. The data agree within 0.3 Å except where extensive motion of the protons is involved. The ‡ symbol (Tables 3−5) represents an intermolecular interaction.

Conclusions

2D ^{1}H−^{13}C HETCOR spectra of natural abundance amino acids and peptides can offer extensive structural information. For our data, the line widths in the ^{13}C dimension were typically 0.4−1.0 ppm (40−100 Hz), whereas the line widths in the proton dimension ranged from 0.5 to 2.0 ppm. The cross peaks in the spectra offer improved resolution and help in the assignment of carbon spectra; more significantly, they can be used to identify the intermolecular hydrogen bonding partners which could not be identified by 1D spectra. Apparently, spectra taken at higher field are more useful in getting that information.

We have used the volumes of those cross peaks to measure the distances between carbons and protons. The accuracy of this measurement is strongly affected by the motions of certain functional groups, including methyl (CH_3) and amine (NH_3^+) groups. Motion on the microsecond time scale can make the polarization transfer very inefficient and weakens the cross peaks. For these groups a careful choice of pulse length and temperature might assist in obtaining the desired information. For the other correlations the relation between cross peak volume (for short mixing times) and distance ($1/r^3$) was linear with standard deviation of 0.2 Å as shown in Figure 8. We failed to find cross peaks from spin pairs with C−H separations larger than 3 Å. Longer range distance correlations would be expected if the proton−proton spin diffusion occurs during the WIM transfer.

In summary, 2D ^{1}H−^{13}C HETCOR shows considerable promise for characterizing hydrogen bond networks, nonbonded interactions, for crude estimates of C−H distances, and for assignments of carbon spectra in complex systems.

Acknowledgment. This research has been supported by a grant from the International Human Frontiers Research Program. The solid state NMR instrument is funded by a grant from the National Science Foundation (NSF CHE-9401988). A.M. acknowledges support from Kanagawa Academy of Science and Technology. The authors are also grateful for the technical support of Chemagnetics, Inc., Fort Collins, CO.

JA952130R